# Dynamic optical response of an excitonic quantum dot studied by solving the self-consistent Maxwell-Schrödinger equations nonperturbatively

S. Hellström and Y. Fu

*Department of Theoretical Chemistry, School of Biotechnology, Royal Institute of Technology, S-106 91 Stockholm, Sweden*
(Received 2 June 2010; revised manuscript received 30 September 2010; published 7 December 2010)

The optical excitation of a quantum dot in real-world working conditions is studied by self-consistent solution of the time-dependent Schrödinger equation coupled to the Maxwell equations by the finite-difference time domain method, resulting in a polarization modification which is the basis for the enhanced light-matter interaction in many nanoscale devices. The commonly used perturbational analysis approach is compared to the results and found to be an acceptable approximation even for intense femtosecond pulse excitations where using the perturbative approach is risky. This allows device designers and simulators to confidently use the simpler and faster perturbative results in their work.

## I. INTRODUCTION

Excitonic resonances can, by coupling with light to form exciton polaritons, significantly affect the dielectric constant—making possible both ultrahigh and negative dielectric constants.[1,2] This would allow improvements in designing novel nanoscale photonic components with high integration density and new functionality. Exciton polaritons in bulk and simple quantum wells were carefully studied during the 1960–70s by stead-state perturbation theories and by now their effects on the optical properties are quite well established, see, e.g., the dedicated volume.[3]

There has been a revival in interest recently with the focus at exciton polaritons in state-of-art nanostructures due to the enhanced light-matter interaction in many nanoscale device designs.[4] This is especially pronounced in semiconductor quantum dots (QDs) where the high confinement factor leads to strong light-matter interaction.

A tractable application path is to build photonic crystals out of QD arrays, which will create photonic and polaritonic band gaps.[5] Such band gaps have been experimentally observed[6] in CdS QDs embedded in face-centered-cubic porous silica matrices. Furthermore, the reflection off a planar InAs QD array in GaAs has been both theoretically and experimentally shown to be high around the QD exciton energy.[7] One-dimensional photonic crystals based on multiple quantum wells (QWs) were shown to be characterized by the presence of a larger-than-usual polariton stop band when the distance between the QWs satisfies the resonance Bragg condition.[8] The exciton-polariton modes at finite in-plane momentum of a QD lattice embedded in a planar optical cavity were shown to be capable of being guided with long lifetimes.[9]

In almost all potential applications of QD exciton polariton, the excitation and recombination processes are expected to be fast and strong. Ultrafast femtosecond (fs) lasers with a peak power as high as 30 GW/cm$^2$ are widely used[10] in multiphoton microscopies to probe the structure and function of neuronal circuits from animals, electron-hole dynamics in semiconductors, coherent transient excitation in atoms and molecules, and nonlinear processes in fibers and guided wave structures.[11] And in concentrated solar cell application, the continuous-wave solar power can also reach the GW/cm$^2$ magnitude. Under all these application circumstances, steady-state perturbation theories could be expected to break down.

Efforts have been made to extend the description of dynamic excitonic properties of QDs from perturbation theories for weak excitation. Electromagnetic simulations of the exciton-polariton influence on the optical properties of QDs have been performed using the finite-difference time domain (FDTD) method.[12] However this and a few other previous efforts[13,14] use several simplifying assumptions, the two main of them being use of perturbation analysis and the negligence of the influence of the exciton polariton on the external excitation radiation field. Furthermore, no attempts on error analysis whatsoever have been done, thus restricting the applicability of these works to low-intensity illumination. The goal of this work is to check the validity of those approximations in real-world device working conditions with intense illumination by comparing the approximations with a reference nonperturbative self-consistent quantum simulation in the time domain, to find basic recommendations for practical QD exciton polariton simulations.

## II. THEORETICAL CONSIDERATIONS

External electromagnetic fields impinging on a QD at its initial state $\Psi_0$ will photoexcite an exciton described by the wave function $\Psi_n(\mathbf{r}_e, \mathbf{r}_h)$, where $\mathbf{r}_e$ denotes the position of the conduction-band electron and $\mathbf{r}_h$ the valence-band hole that together forms the exciton. The initial QD state $\Psi_0$ is normally without any excitons and its energy is referred to be $\hbar\omega_0 = \langle\Psi_0|H_0|\Psi_0\rangle = 0$, while the energy of exciton state $n$ is $\langle\Psi_n|H_0|\Psi_n\rangle = \hbar\omega_n$. Here $H_0$ denotes the Hamiltonian of electrons in the QD. The exciton's interaction with an external electromagnetic field $\mathbf{E}(\mathbf{r}, t)$ is described by the additional Hamiltonian

$$H_1(t) = \int \mathbf{d}(\mathbf{r}) \cdot \mathbf{E}(\mathbf{r}, t) d\mathbf{r}, \tag{1}$$

where $\mathbf{d}(\mathbf{r}) = -e\mathbf{r}_e\delta(\mathbf{r} - \mathbf{r}_e) + e\mathbf{r}_h\delta(\mathbf{r} - \mathbf{r}_h)$ is the dipole moment operator of the exciton and $e$ the unit charge.

We now consider the two-state system of $\Psi_0$ and $\Psi_n$ coupled by $H_1$ and express the time-dependent wave function as

$$|r_e, r_h, t\rangle = c_0(t)|\Psi_0(r_e, r_h)\rangle + c_n(t)|\Psi_n(r_e, r_h)\rangle. \quad (2)$$

We only concern ourselves with two states as it has been shown that in real-world applications, further excited state populations are very small as to be negligible.[15] Additionally, we will see later that the population modifications due to the external electromagnetic field are very small so that high-energy states are not relevant from the numerical point of view.

Solving numerically the time-dependent Schrödinger equation is best approached through the Cayley form[16,17] which preserves the wave function's energy over time better than the straightforward finite-difference approach often used

$$\left[1 + \frac{i\delta}{2\hbar}H(r, t+\delta)\right]|r_e, r_h, t+\delta\rangle = \left[1 - \frac{i\delta}{2\hbar}H(r, t)\right]|r_e, r_h, t\rangle, \quad (3)$$

where $H = H_0 + H_1$. This becomes the well-known Crank-Nicholson scheme if the spatial differentials in the Hamiltonian are expanded by finite differences but here we already know the wave function and the expectation values so we keep the real-space part analytical and only expand the time part. By expanding Eq. (3), using $H_0|\Psi_0\rangle = 0$, $H_0|\Psi_n\rangle = \hbar\omega_n$, and $\langle\Psi_n|H_1|\Psi_n\rangle = 0$, we get

$$c_0(t+\delta) + \frac{i\delta}{2\hbar}[c_n(t+\delta)\langle\Psi_0|H_1(t+\delta)|\Psi_n\rangle] = c_0(t) - \frac{i\delta}{2\hbar}[c_n(t)$$
$$\times\langle\Psi_0|H_1(t)|\Psi_n\rangle], \quad (4)$$

$$c_n(t+\delta) + \frac{i\delta}{2\hbar}[c_n(t+\delta)\hbar\omega_n + c_0(t+\delta)\langle\Psi_n|H_1(t+\delta)|\Psi_0\rangle]$$
$$= c_n(t) - \frac{i\delta}{2\hbar}[c_n(t)\hbar\omega_n + c_0(t)\langle\Psi_n|H_1(t)|\Psi_0\rangle] \quad (5)$$

from which we can obtain $c_0(t+\delta)$ and $c_n(t+\delta)$ from $c_0(t)$ and $c_n(t)$. We emphasize that these expressions contain the full nonlinear behavior of the system—the final polarization term will depend nonlinearly on the $E$ field and is not linear.

Through the use of second quantization, the matrix elements in the above equation can be evaluated[5]

$$\langle\Psi_n(r_e, r_h)|d(r)|\Psi_0(r_e, r_h)\rangle = \frac{ep_{cv}}{\omega_n m_0}\psi_n(r, r)\langle\Psi_n(r_e, r_h)$$
$$\times|\int p_e \cdot E(r_e, t)dr|\Psi_0(r_e, r_h)\rangle$$
$$= \frac{e}{\omega_n m_0}\int \psi_n^*(r, r)p_{cv} \cdot E(r, t)dr, \quad (6)$$

where $p_{cv} = \langle c|p|v\rangle$ is the dipole momentum between conduction and valence bands, $m_0$ is the free electron mass, and $\psi_n(r_e, r_h)$ is the exciton envelope function which is known analytically for a perfectly spherical QD.

After acquiring $c_0(t)$ and $c_n(t)$, the polarization due to the exciton excitation can be easily calculated by

$$P(r, t) = \langle r_e, r_h, t|d(r)|r_e, r_h, t\rangle. \quad (7)$$

Such a polarization will affect the incident electromagnetic field governed by the time evolution of the Maxwell equations

$$\frac{\partial E}{\partial t} = \frac{1}{\epsilon_r\epsilon_0}\left(\nabla \times H - \frac{\partial P}{\partial t}\right),$$

$$\frac{\partial H}{\partial t} = -\frac{1}{\mu_r\mu_0}\nabla \times E, \quad (8)$$

where $\epsilon_0$ and $\mu_0$ are permittivity and permeability of free space, respectively, $\epsilon_r$ and $\mu_r$ are relative dielectric and magnetic constants of the material under investigation.

By Eqs. (4) and (5) it is easy to obtain

$$\frac{\partial P(r, t+\delta)}{\partial t} = \frac{iep_{cv}}{m_0}\psi_n(r, r)[c_n^*(t)c_0(t) - c_n(t)c_0^*(t)]. \quad (9)$$

In our numerical implementation we use the standard FDTD method[18,19] to evolve the electromagnetic fields $E(r, t)$ and $H(r, t)$ in time, and at each time step $c_0(t)$, $c_n(t)$ and thus $\partial P(r, t)/\partial t$ are updated by Eqs. (4) and (9), taking care to keep units consistent between the two parts of the calculation. By this electromagnetic-quantum mechanical coupling, we achieve self-consistent simulations of the exciton-polariton effects due to its modification of the optical near field inside the QD.

We have made two major approximations thus far: The first one is that Eq. (1) neglects the $E^2$ term which has been shown to be valid for QDs even when illuminated by ultraintense fs laser pulses.[15] $E^2$ terms only matter when the transitions induced by the linear term are forbidden. Nonlinear phenomena such as two-photon absorption and the optical Kerr effect will still appear without this term and the change to two-photon absorption due to the $E^2$ term has shown to be negligible.[20] The resulting polarization is not expanded into terms of $E$ so we keep almost full nonlinearity of $E$.

Equation (2) makes the second approximation which assumes that high-energy states are not relevant as the occupations are very small as it has been shown[15] that the ratio of high-energy exciton state occupations can be as small as $10^{-10}$. This can be easily made more precise by adding more states when the population distributions in high-energy states become nontrivial but due to the fast relaxation processes in InAs QDs, the improvement is expected to be negligible. Equation (9) should thus be a good approximation when coupled with the Maxwell equations Eq. (8).

A third common approximation is to assume that $|c_n| \ll 1$ or $\partial|c_n|/\partial t \approx 0$, which allows the use of perturbative analysis as the ground state (unexcited) occupation can be approximated to be unity at all times. Some articles (e.g., Ref. 2) have used an expression for the dielectric constant which is obtained by constructing a linear response function by neglecting the contribution of the excitonic polarization to the total electromagnetic field, taking $\epsilon_r E(r, \omega) + P(r, \omega) \approx \epsilon_{QD}(r, \omega)E(r, \omega)$. This is equivalent to decoupling the
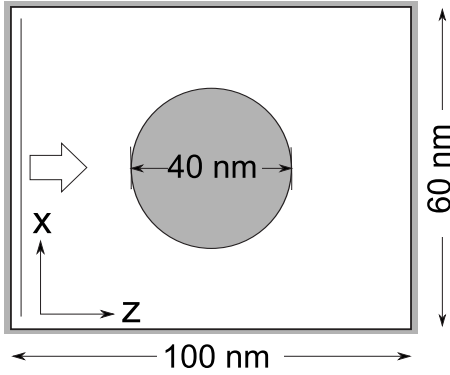
FIG. 1. Schematic of the geometry used in the simulations.



FIG. 2. (a) $yz$ plane cross-section view of the $|P|$ polarization in the QD (marked by dotted circle).

quantum-mechanical calculation of the light-matter interaction from the electrodynamical simulation.

As the QDs are normally much smaller than the wavelength of the incoming light, the $E$ field is often assumed to be uniform inside the QD. For this work, we simply use the $E$ field value at the center of the QD to test this approximation.

The aim of this work is to check the validity of the three last approximations. This is achieved by performing nonperturbative calculations with full self-consistency, using Eqs. (4) and (9), and then a set of calculations using the dynamics and polarization obtained by perturbation analysis, with the two other approximations enabled or disabled.

## III. RESULTS AND DISCUSSIONS

As we are mostly interested in verifying the accuracy of the various approximations in real-world situations, we limit our investigation to two popular applications at the extremes of excitation intensities: excitation due to an intense fs laser pulse and excitation due to solar radiation.

The relation between the incident radiation power $I$ and the electric field strength in monochromatic plane wave radiation with average electric field amplitude $E$ is $I = c\epsilon_r\epsilon_0 E^2/2$, where $c$ is the speed of light. The average peak solar radiation power at the ground is $I \approx 1400$ W/m$^2$ which can induce an average electric field of $E_{solar} = 10^3$ V/m in common semiconductors for which the dielectric constant is usually $\epsilon_r \approx 10$. On the other hand, common fs lasers can generate a peak power as high as $10^{10}$ W/m$^2$, which gives $E_{fs} = 2.75 \times 10^6$ V/m.

We examine a single 20 nm radius InAs QD embedded in a GaAs matrix. For InAs QDs of the radius used, the exciton resonance frequency is $\hbar\omega_n = 0.417$ eV and the dielectric constant is $\epsilon_\infty = 15.0$. The direction of the crystal momentum $p_{cv}$ is usually random for QDs, we here use the unit direction $(1,1,1)$ for simplicity.

The FDTD lattice grid is $60 \times 60 \times 100$ nm$^3$ large with a mesh size of 1.0 nm. The lattice is assumed to be filled of GaAs material with dielectric constant $\epsilon = 13.0$ and the InAs QD is positioned at the center. The boundaries of the simulation space are set to be perfectly absorbing in order to remove spurious reflections by the perfectly matched layers method.[19] This setup is sketched in Fig. 1.
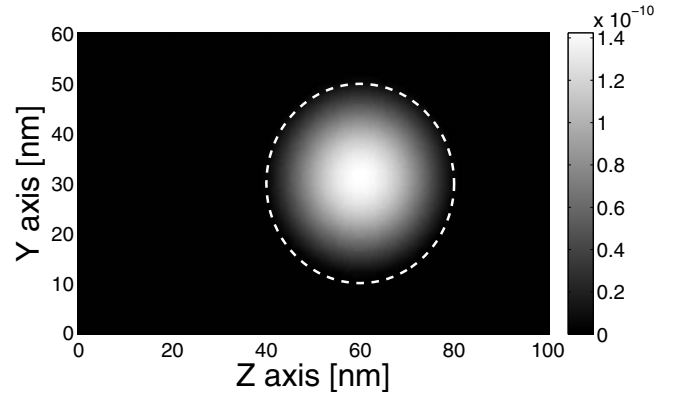
The source in the FDTD simulation emits a single-TE ($E_z = 0$) mode pulse propagating along the $+z$ direction, with a center frequency of $\omega = 2.28 \times 10^{15}$ Hz (corresponding to the exciton resonance energy) and a pulse frequency bandwidth of 10% of the center frequency. The amplitude is set to be one of the two excitation intensities $E_{solar}$ or $E_{fs}$.

At each step in the full self-consistent nonperturbative calculation, the populations $c_0$ and $c_1$ are normalized to fulfil $|c_0|^2 + |c_1|^2 = 1$, in order to avoid numerical errors and ensure long-term stability. We first study the fs laser case as its higher excitation intensity makes it more susceptible to approximation errors and will thus exhibit errors more clearly than the solar cell case.

Figure 2 shows a resulting polarization $|P|$ in a $y$-$z$ cross-section plane view through the middle of the simulation volume. The $|E|^2$ field from the full self-consistent solution just after the end of the excitation is shown in Fig. 3 together with the error that arises when the resulting polarization is not fed back to the electrodynamics calculations. Without the EM-QM coupling, $E_z$ is much smaller and only exhibit the frequency-independent dielectric response from the slight difference in index of refraction between the QD material and the surrounding material.

Note that the self-consistent $E$ field strength is much smaller compared to the external excitation of $10^6$ V/m. This is an initial indication that the nonself-consistent approximation may be valid even for intense fs laser pulses. The $|E_z|^2$ field is shown in Fig. 4, demonstrating the variation of the polarization-generated $E$ field inside the QD and also the dependence on the crystal momentum direction $p_{cv}$. It is clear from the figure that the direction of the polarization lies along the same direction as $p_{cv}$.
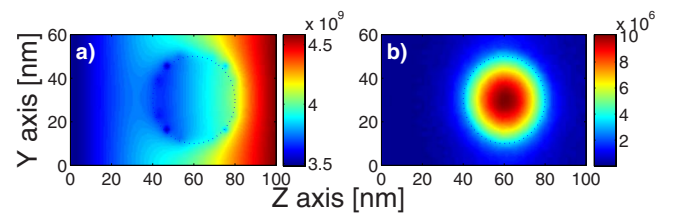


FIG. 3. (Color online) (a) $yz$ plane cross-section view of the $|E|^2$ field close to the QD (marked by dotted circle). (b) The absolute error in $|E|^2$ calculated perturbatively without self consistency.
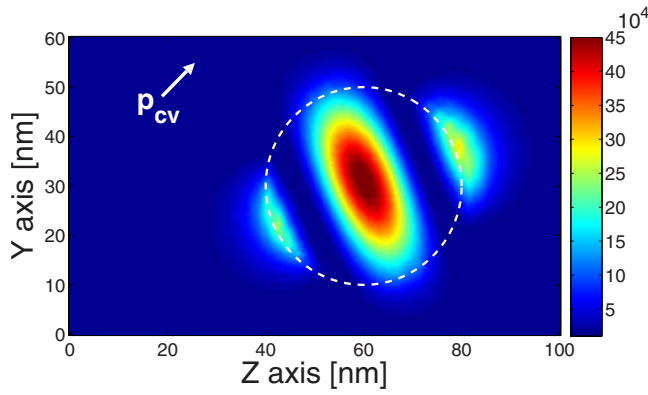
FIG. 4. (Color online) (a) $yz$ plane cross-section view of the $|E_z|^2$ field close to the QD (marked by dotted circle).

In Fig. 5, the $|E_z|^2$ along the $z$ axis for the full solution is shown with the $|E_z|^2$ field when there is no self-consistency shown magnified, exhibiting the pure dielectric response. This is similar to what has been observed in Ref. 12 and demonstrates that while most of the exciton contributions to the $E$ field occur deep inside the QD, there are spots on the QD surface with a smaller but still significant field magnitude.

The population dynamics obtained by both the full self-consistent and the perturbative simulations are shown in Fig. 6. The curves turn out to be so close to each other as being not distinguishable in the figure. Due to the small frequency width, the pulse rise time is long which causes the apparent delay in the figures. The actual exciton polariton response is very quick, with response time shorter than what can be distinguished. Figure 6 shows that the excitation probability $|c_n|^2$ remains very small so that the two-state approximation used is acceptable and also the simple perturbational analysis disregarding the population changes in the ground state.

Figure 7 shows the relative error in the approximate calculations of $|c_n|^2$ compared to the nonperturbative self-consistent solution. It turns out that the error is around one per mil for the various approximations. Thus other external and experimental error sources are likely to completely overwhelm the error from taking the simpler approaches to calculate the excitonic polarization when performing experi-
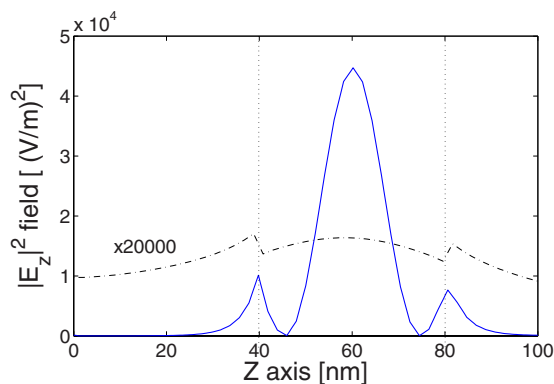


FIG. 5. (Color online) $|E_z|^2$ field along the $z$ axis. For comparison purposes, the nonself-consistent field is shown magnified 20 000 times and vertical lines mark the extents of the QD.
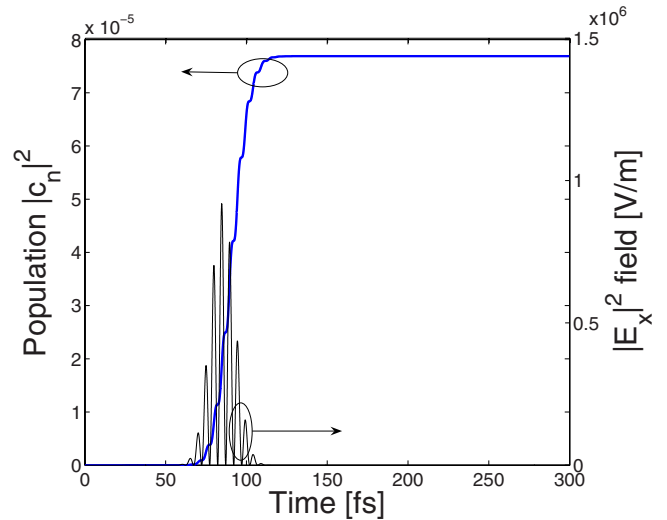


FIG. 6. (Color online) Population dynamics of first excited state with fs laser pulse $E$ field shown for comparison.

ments. We also see that the assumptions of nonself-consistency and of uniform $E$ field contribute roughly equally to the error and that those two approximations are much larger than the perturbative approximation.

The dynamics of the polarization at the center of the QD is shown in Fig. 8. The difference between the self-consistent and perturbative solutions turns out to be very small too with the only difference being a slight difference in amplitude. There is no delay in the excitation when comparing the self-consistent and perturbative solutions, as could be expected. The error in $P$ for the various approximations is shown in Fig. 9, where it is clear that the error is very small.

We now briefly explore a case where the perturbative approach can be expected to have a lot of trouble. In Fig. 10 the excited population is shown for pumped QDs, i.e., QDs with a part of its population already excited prior to the additional excitation in the simulation. A such situation is common in light-emitting devices and particularly lasers and it is a case
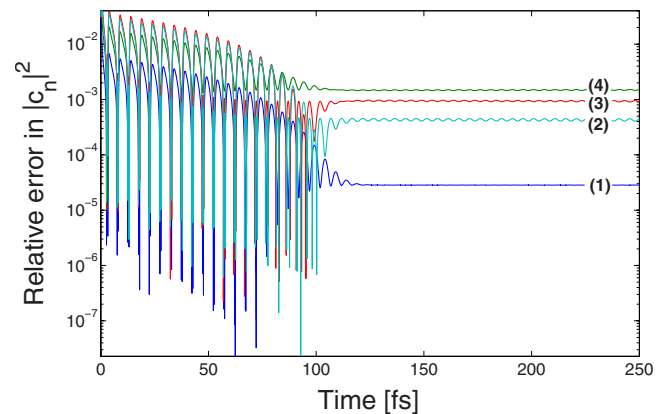


FIG. 7. (Color online) Relative error in the population compared to full self-consistent solution. Curve (1) refers to perturbative calculation with self-consistency and nonuniform $E$ field, (2) nonperturbative calculation with self-consistency but uniform $E$ field, (3) perturbative nonself-consistent with uniform $E$ field, and (4) perturbative nonself-consistent but with nonuniform $E$ field.
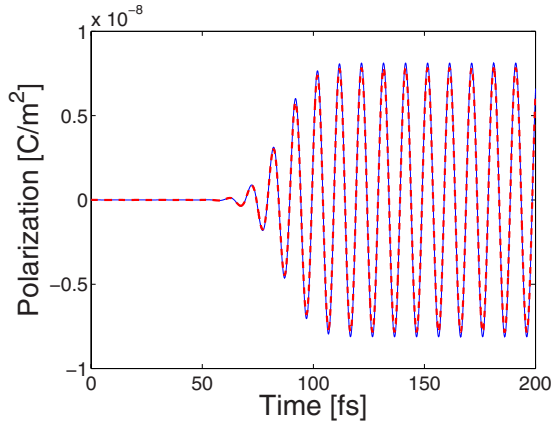
FIG. 8. (Color online) Polarization dynamics at the center of the QD for fs laser case. Red dashed curve is for the calculation with all three approximations enabled.

where the $|c_0|^2 = 1.0$ assumption breaks down.

For an initial population of $|c_0|^2 = 0.64$, the relative error shown in Fig. 11 is under one percent, indicating again that the agreement is good but not as excellent as the earlier results as the relative error now approaches one percent. Thus the perturbational method without self-consistency is mostly appropriate for systems of initially unexcited dots but can simulate pumped QDs if the moderately increased error is acceptable.

We have hitherto done comparisons mostly in time domain rather than frequency domain because of the extremely narrow excitonic frequency response (which is around the order of the exciton longitudinal-transverse splitting frequency, $\hbar\omega_{LT} = 0.03$ meV). Due to the time-frequency uncertainty relation inherent in time-frequency transforms, unfeasibly long simulation durations would be needed to obtain the desired precision (preferably around $\omega_{LT}/100$). A number of workaround methods like the Padé approximation[21] exist
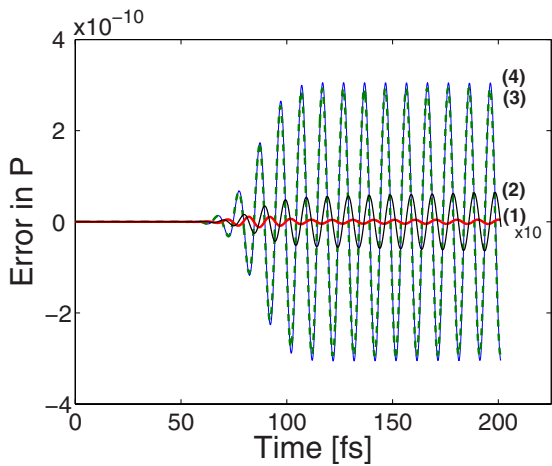


FIG. 9. (Color online) Error in the polarization dynamics. The tenfold magnified curve (1) refers to the case with perturbative calculation using EM feedback and nonuniform $E$ field. Curve (2) shows the nonperturbative solution with feedback but uniform $E$ field. Curves (3) and (4) are from perturbative nonself-consistent calculations with uniform and nonuniform $E$ fields, respectively.
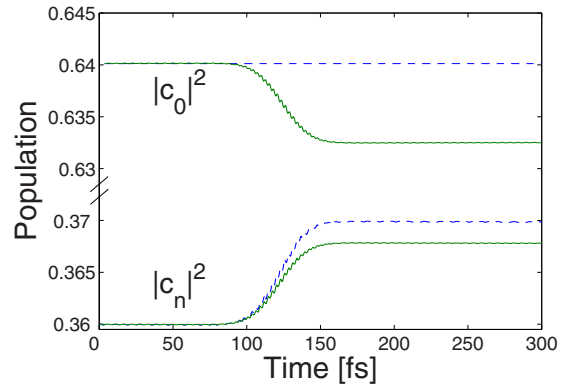


FIG. 10. (Color online) Pumped population dynamics. Note that there is a jump in the vertical axis.

that can increase the resolution but they do not provide sufficient precision to allow obtaining the real/imaginary parts of the dielectric constant's dispersion curves, making detailed comparisons difficult. The methods do however excel in finding the poles of a system and can thus show resonance shifts, widths, and $Q$ factors.

In Fig. 12 we show how the resonant frequency moves slightly for the solution without approximations, where we have used the Padé method to obtain the pole of the simulated QD. The approximate solution has its pole exactly where expected, at the resonance frequency $\omega_n$ but when the polarization is fed back to the EM calculations the resonance shifts a little bit. This shift is much smaller than the $0.3\omega_{LT}$ shift observed in QD lattices[12] so the self-contribution to the resonance shift can safely be ignored for most cases.

The solar radiation case turns out to be very similar as the femtosecond case but with a smaller relative error of approximately $10^{-5}$ for the population. This result is as expected since the energy due to nonconcentrated solar illumination is as small as to be comfortably modeled as perturbative.

## IV. SUMMARY

The perturbative approach is a popular way to simplify complex optical phenomena into expressions easily used to
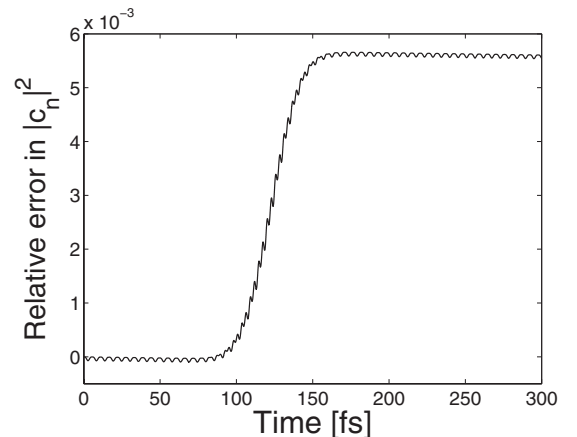


FIG. 11. Relative error in the pumped population dynamics.
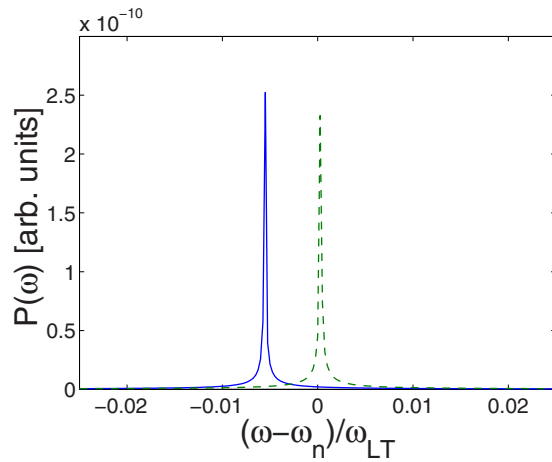
FIG. 12. (Color online) Resonance frequency shifts for polarization. Blue whole curve is the full solution while green dashed curve is for the case with all three approximations enabled.

design and simulate photonic components but always with the caveat of it being a rather crude approximation that could be expected to break down in a few specialized applications. Intense femtosecond pulses are one of those applications since the perturbation term applied is ultrahigh and only applied in a very short time scale. Thus prior to our work, naïvely applying perturbational analysis to quantum dot femtosecond excitation has been fraught with the risk that it might not properly model the population dynamics and therefore the resulting polarization. Using self-consistent nonperturbative Maxwell-Schrödinger solvers is nontrivial and rather slow. Many FDTD codes only support simple Lorentz-like dispersion models and it is desirable to be able to use the simplified expressions found for the permittivity[7] which is obtained directly from the analytical expressions from the perturbative approach.

We have, by using a self-consistent nonperturbative approach to solving the Maxwell-Schrödinger equations, shown that the perturbative approach turns out to be satisfactory for analyzing real-world femtosecond device designs. Furthermore, the approximation that the excitonic polarization does not significantly affect the local $E$ field is valid, and also the assumption that the $E$ field is uniform inside the QD. The perturbative approach turns out to be a very acceptable approximation even for intense femtosecond applications as the error is smaller than what can be expected to arise from external error sources such as fabrication irregularities. Knowing this, device designers can in the future confidently use the expression for the exciton polariton-induced permittivity obtained by perturbational analysis, even for the intense femtosecond pulse regime.

## ACKNOWLEDGMENTS

[1] R. Zia, J. A. Schuller, A. Chandran, and M. L. Brongersma, Mater. Today **9**, 20 (2006).

[2] Y. Fu, L. Thylén, and H. Ågren, Nano Lett. **8**, 1551 (2008).

[3] *Excitons*, edited by M. D. Sturge and E. I. Rashba (North-Holland, Amsterdam, 1982).

[4] Y. Fu, S. Hellström, and H. Ågren, J. Nonlinear Opt. Phys. Mater. **18**, 195 (2009).

[5] Y. Fu, M. Willander, and E. L. Ivchenko, Superlattices Microstruct. **27**, 255 (2000).

[6] Y. A. Vlasov, V. N. Astratov, O. Z. Karimov, A. A. Kaplyanskii, V. N. Bogomolov, and A. V. Prokofiev, Phys. Rev. B **55**, R13357 (1997).

[7] Y. Fu, H. Ågren, L. Höglund, J. Y. Andersson, C. Asplund, M. Qiu, and L. Thylén, Appl. Phys. Lett. **93**, 183117 (2008).

[8] E. L. Ivchenko, M. M. Voronov, M. V. Erementchouk, L. I. Deych, and A. A. Lisyansky, Phys. Rev. B **70**, 195106 (2004).

[9] E. M. Kessler, M. Grochol, and C. Piermarocchi, Phys. Rev. B **77**, 085306 (2008).

[10] S. A. Blanton, A. Dehestani, P. C. Lin, and P. Guyot-Sionnest, Chem. Phys. Lett. **229**, 317 (1994).

[11] *Femtosecond Laser Pulses: Principles and Experiments*, 2nd ed., edited by C. Rulliére (Springer, New York, 2005.

[12] Y. Zeng, Y. Fu, M. Bengtsson, X. Chen, W. Lu, and H. Ågren, Opt. Express **16**, 4507 (2008).

[13] A. Bratkovsky, E. Ponizovskaya, S.-Y. Wang, P. Holmström, L. Thylén, Y. Fu, and H. Ågren, Appl. Phys. Lett. **93**, 193106 (2008).

[14] Y. Fu, E. Berglind, L. Thylén, and H. Ågren, J. Opt. Soc. Am. B **23**, 2441 (2006).

[15] Y. Fu, T.-T. Han, Y. Luo, and H. Ågren, J. Phys.: Condens. Matter **18**, 9071 (2006).

[16] A. Goldberg, H. M. Schey, and J. L. Shwartz, Am. J. Phys. **35**, 177 (1967).

[17] Y. Hou, W.-P. Wang, N. Li, W.-L. Xu, W. Lu, and Y. Fu, Appl. Phys. Lett. **93**, 132108 (2008).

[18] K. Yee, IEEE Trans. Antennas Propag. **14**, 302 (1966).

[19] A. Taflove and S. C. Hagness, *Computational Electrodynamics: The Finite-Difference Time-Domain Method*, 2nd ed. (Artech House, Boston, 2000).

[20] A. Gold and J. P. Hernandez, Phys. Rev. **139**, A2002 (1965).

[21] S. Dey and R. Mittra, IEEE Microw. Guid. Wave Lett. **8**, 415 (1998).